

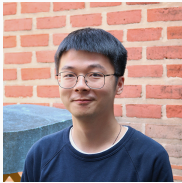
Comparing the robustness of different high order entropy stable discontinuous Galerkin methods

Jesse Chan

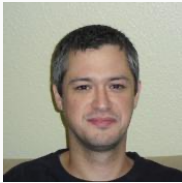
Dept. of Computational and Applied Mathematics
Rice University

New Trends in Numerical Methods for Hyperbolic Conservation Laws
Purdue University

Collaborators



Yimin Lin (Euler,
compressible NS)



Ignacio Tomas



Philip (Xinhui) Wu



Nathaniel Trask



Hendrik Ranocha



Andres
Ruéda-Ramírez



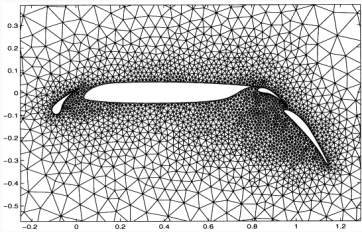
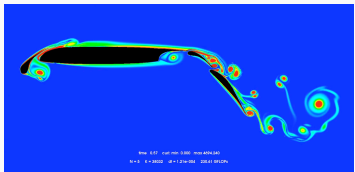
Gregor Gassner



Tim Warburton

High order finite element methods for hyperbolic PDEs

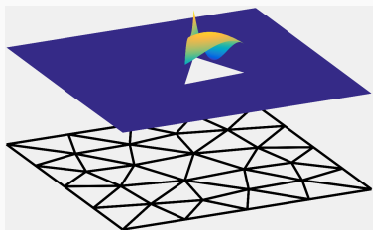
- Aerodynamics applications:
acoustics, vorticular flows,
turbulence, shocks.
- Goal: **high accuracy** on
unstructured meshes.
- Discontinuous Galerkin
(DG) methods: geometric
flexibility + high order.



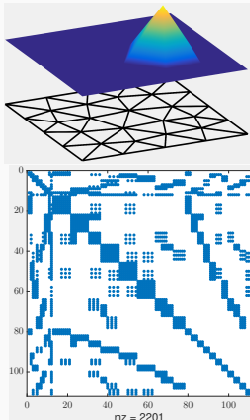
Mesh from Slawig 2001.

High order finite element methods for hyperbolic PDEs

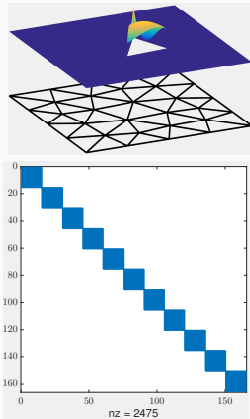
- Aerodynamics applications:
acoustics, vorticular flows,
turbulence, shocks.
- Goal: **high accuracy** on
unstructured meshes.
- Discontinuous Galerkin
(DG) methods: geometric
flexibility + high order.



Why discontinuous Galerkin methods?



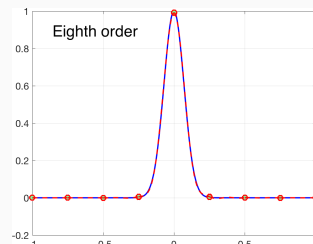
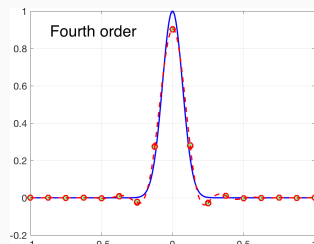
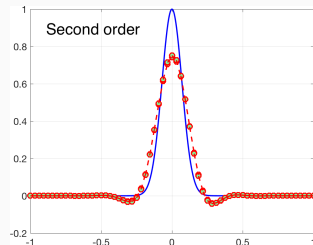
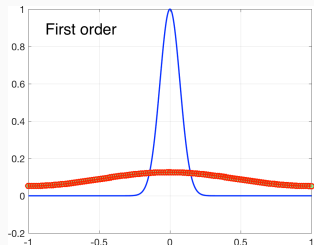
(a) High order FEM



(b) High order DG

High order DG mass matrices: easily invertible for **explicit time-stepping**.

Why high order accuracy?



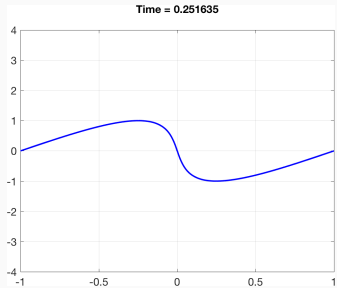
Accurate resolution of propagating vortices and waves.

Why high order accuracy?

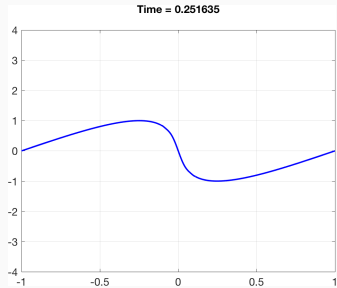


2nd, 4th, and 16th order Taylor-Green vortex. Vorticlar structures and acoustic waves are both sensitive to numerical dissipation.

Why *not* high order DG methods?



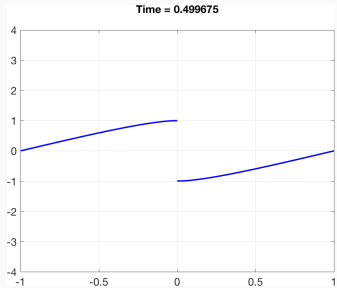
(a) Exact solution



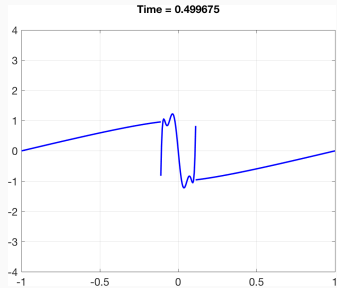
(b) 8th order DG

High order methods blow up for under-resolved solutions of nonlinear conservation laws (e.g., shocks and turbulence).

Why *not* high order DG methods?



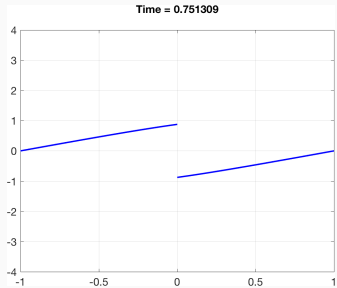
(a) Exact solution



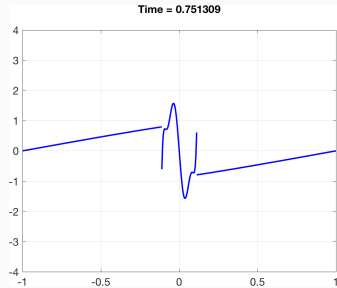
(b) 8th order DG

High order methods blow up for under-resolved solutions of nonlinear conservation laws (e.g., shocks and turbulence).

Why *not* high order DG methods?



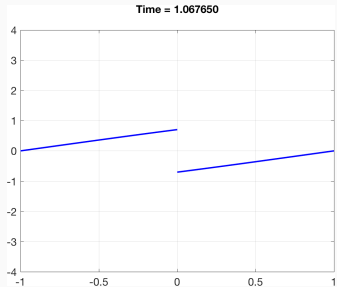
(a) Exact solution



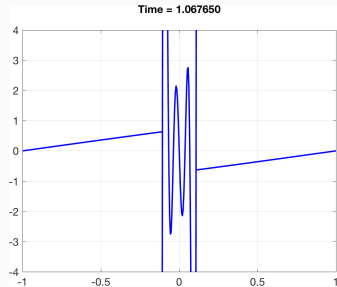
(b) 8th order DG

High order methods blow up for under-resolved solutions of nonlinear conservation laws (e.g., shocks and turbulence).

Why *not* high order DG methods?



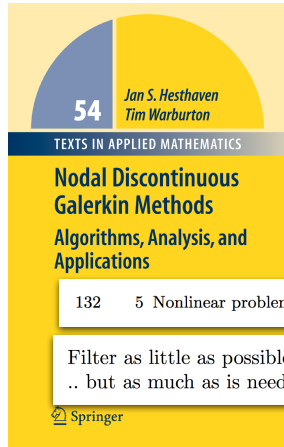
(a) Exact solution



(b) 8th order DG

High order methods blow up for under-resolved solutions of nonlinear conservation laws (e.g., shocks and turbulence).

Why entropy stability for high order schemes?



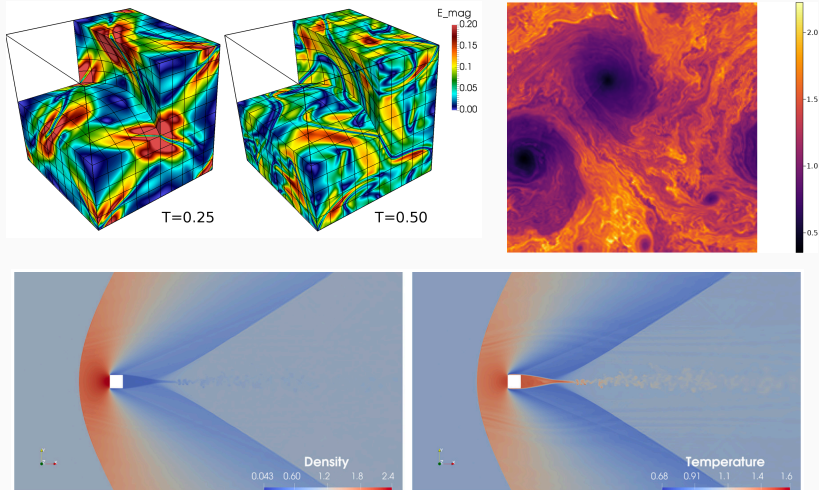
- High order DG needs heuristic stabilization (e.g., artificial viscosity, filtering).
- Entropy stable schemes improve robustness without adding extra dissipation.
- Turns DG into a “good” high order method (though not 100% bulletproof).

Finite volume methods: Tadmor, Chandrashekar, Ray, Svard, Fjordholm, Mishra, LeFloch, Rohde, ...

High order tensor product elements: Fisher, Carpenter, Gassner, Winters, Kopriva, Persson, ...

High order general elements: Chen and Shu, Crean, Hicken, Del Rey Fernandez, Zingg, ...

Examples of high order entropy stable simulations



All simulations are ESDG without artificial viscosity, filtering, or slope limiting.

Bohm et al. (2019). *An entropy stable nodal DG method for the resistive MHD equations. Part I.*

Dalcin et al. (2019). *Conservative and ES solid wall BCs for the compressible NS equations.*

Talk outline

1. From entropy stable finite volumes to entropy stable nodal DG
 - 1.1 “Modal” entropy stable DG formulations
2. Positivity preserving entropy stable nodal DG for the compressible Navier-Stokes equations
3. Differences in robustness for different entropy stable schemes

From entropy stable finite volumes to entropy stable nodal DG

Entropy stability for nonlinear problems

- Energy balance for **nonlinear** conservation laws (Burgers', shallow water, compressible Euler + Navier-Stokes).

$$\frac{\partial \mathbf{u}}{\partial t} + \frac{\partial \mathbf{f}(\mathbf{u})}{\partial x} = 0.$$

- Continuous entropy inequality: convex **entropy** function $S(\mathbf{u})$, “entropy potential” $\psi(\mathbf{u})$, entropy variables $\mathbf{v}(\mathbf{u})$

$$\int_{\Omega} \mathbf{v}^T \left(\frac{\partial \mathbf{u}}{\partial t} + \frac{\partial \mathbf{f}(\mathbf{u})}{\partial x} \right) = 0, \quad \boxed{\mathbf{v}(\mathbf{u}) = \frac{\partial S}{\partial \mathbf{u}}} \\ \Rightarrow \int_{\Omega} \frac{\partial S(\mathbf{u})}{\partial t} + \left(\mathbf{v}^T \mathbf{f}(\mathbf{u}) - \psi(\mathbf{u}) \right) \Big|_{-1}^1 \leq 0.$$

Entropy conservative finite volume methods

- Finite volume scheme:

$$\frac{d\mathbf{u}_i}{dt} + \frac{\mathbf{f}_S(\mathbf{u}_{i+1}, \mathbf{u}_i) - \mathbf{f}_S(\mathbf{u}_{i+1}, \mathbf{u}_i)}{h} = \mathbf{0}.$$

- Take \mathbf{f}_S to be an **entropy conservative** numerical flux

$$\mathbf{f}_S(\mathbf{u}, \mathbf{u}) = \mathbf{f}(\mathbf{u}), \quad (\text{consistency})$$

$$\mathbf{f}_S(\mathbf{u}, \mathbf{v}) = \mathbf{f}_S(\mathbf{v}, \mathbf{u}), \quad (\text{symmetry})$$

$$(\mathbf{v}_L - \mathbf{v}_R)^T \mathbf{f}_S(\mathbf{u}_L, \mathbf{u}_R) = \psi_L - \psi_R, \quad (\text{conservation}).$$

- Can show numerical scheme **conserves** entropy

$$\int_{\Omega} \frac{\partial S(\mathbf{u})}{\partial t} \approx \sum_i h \frac{dS(\mathbf{u}_i)}{dt} = 0.$$

Entropy stable finite volume methods

- Finite volume scheme with dissipation term $\mathbf{d}(\mathbf{u})$:

$$\frac{d\mathbf{u}_i}{dt} + \frac{\mathbf{f}_S(\mathbf{u}_{i+1}, \mathbf{u}_i) - \mathbf{f}_S(\mathbf{u}_{i+1}, \mathbf{u}_i)}{h} = \mathbf{d}(\mathbf{u}).$$

- Take \mathbf{f}_S to be an entropy conservative numerical flux

$$\mathbf{f}_S(\mathbf{u}, \mathbf{u}) = \mathbf{f}(\mathbf{u}), \quad (\text{consistency})$$

$$\mathbf{f}_S(\mathbf{u}, \mathbf{v}) = \mathbf{f}_S(\mathbf{v}, \mathbf{u}), \quad (\text{symmetry})$$

$$(\mathbf{v}_L - \mathbf{v}_R)^T \mathbf{f}_S(\mathbf{u}_L, \mathbf{u}_R) = \psi_L - \psi_R, \quad (\text{conservation}).$$

- Can show numerical scheme dissipates entropy

$$\int_{\Omega} \frac{\partial S(\mathbf{u})}{\partial t} \approx \sum_i h \frac{dS(\mathbf{u}_i)}{dt} = \mathbf{v}^T \mathbf{d}(\mathbf{u}) \stackrel{?}{\leq} 0.$$

Matrix reformulation using Hadamard products

Hadamard product of two matrices $\mathbf{A} \circ \mathbf{B}$

$$\begin{bmatrix} \mathbf{A}_{11} & \dots & \mathbf{A}_{1n} \\ \vdots & \ddots & \vdots \\ \mathbf{A}_{n1} & \dots & \mathbf{A}_{nn} \end{bmatrix} \circ \begin{bmatrix} \mathbf{B}_{11} & \dots & \mathbf{B}_{1n} \\ \vdots & \ddots & \vdots \\ \mathbf{B}_{n1} & \dots & \mathbf{B}_{nn} \end{bmatrix} = \begin{bmatrix} \mathbf{A}_{11}\mathbf{B}_{11} & \dots & \mathbf{A}_{1n}\mathbf{B}_{1n} \\ \vdots & \ddots & \vdots \\ \mathbf{A}_{n1}\mathbf{B}_{n1} & \dots & \mathbf{A}_{nn}\mathbf{B}_{nn} \end{bmatrix}.$$

Rewrite an N -point (periodic) finite volume scheme as

$$\frac{d}{dt} \begin{bmatrix} \mathbf{u}_1 \\ \mathbf{u}_2 \\ \vdots \\ \mathbf{u}_N \end{bmatrix} + \frac{1}{h} \begin{bmatrix} f_S(\mathbf{u}_1, \mathbf{u}_2) - f_S(\mathbf{u}_N, \mathbf{u}_1) \\ f_S(\mathbf{u}_2, \mathbf{u}_3) - f_S(\mathbf{u}_1, \mathbf{u}_2) \\ \vdots \\ f_S(\mathbf{u}_N, \mathbf{u}_1) - f_S(\mathbf{u}_{N-1}, \mathbf{u}_N) \end{bmatrix} = \mathbf{0}.$$

Matrix reformulation using Hadamard products

Hadamard product of two matrices $\mathbf{A} \circ \mathbf{B}$

$$\begin{bmatrix} \mathbf{A}_{11} & \dots & \mathbf{A}_{1n} \\ \vdots & \ddots & \vdots \\ \mathbf{A}_{n1} & \dots & \mathbf{A}_{nn} \end{bmatrix} \circ \begin{bmatrix} \mathbf{B}_{11} & \dots & \mathbf{B}_{1n} \\ \vdots & \ddots & \vdots \\ \mathbf{B}_{n1} & \dots & \mathbf{B}_{nn} \end{bmatrix} = \begin{bmatrix} \mathbf{A}_{11}\mathbf{B}_{11} & \dots & \mathbf{A}_{1n}\mathbf{B}_{1n} \\ \vdots & \ddots & \vdots \\ \mathbf{A}_{n1}\mathbf{B}_{n1} & \dots & \mathbf{A}_{nn}\mathbf{B}_{nn} \end{bmatrix}.$$

Rewrite an N -point (periodic) finite volume scheme as

$$\frac{d}{dt} \begin{bmatrix} \mathbf{u}_1 \\ \mathbf{u}_2 \\ \vdots \\ \mathbf{u}_N \end{bmatrix} + \frac{1}{h} \begin{bmatrix} f_S(\mathbf{u}_1, \mathbf{u}_2) - f_S(\mathbf{u}_N, \mathbf{u}_1) \\ f_S(\mathbf{u}_2, \mathbf{u}_3) - f_S(\mathbf{u}_1, \mathbf{u}_2) \\ \vdots \\ f_S(\mathbf{u}_N, \mathbf{u}_1) - f_S(\mathbf{u}_{N-1}, \mathbf{u}_N) \end{bmatrix} = \mathbf{0}.$$

Matrix reformulation using Hadamard products

Hadamard product of two matrices $\mathbf{A} \circ \mathbf{B}$

$$\begin{bmatrix} \mathbf{A}_{11} & \dots & \mathbf{A}_{1n} \\ \vdots & \ddots & \vdots \\ \mathbf{A}_{n1} & \dots & \mathbf{A}_{nn} \end{bmatrix} \circ \begin{bmatrix} \mathbf{B}_{11} & \dots & \mathbf{B}_{1n} \\ \vdots & \ddots & \vdots \\ \mathbf{B}_{n1} & \dots & \mathbf{B}_{nn} \end{bmatrix} = \begin{bmatrix} \mathbf{A}_{11}\mathbf{B}_{11} & \dots & \mathbf{A}_{1n}\mathbf{B}_{1n} \\ \vdots & \ddots & \vdots \\ \mathbf{A}_{n1}\mathbf{B}_{n1} & \dots & \mathbf{A}_{nn}\mathbf{B}_{nn} \end{bmatrix}.$$

Rewrite an N -point (periodic) finite volume scheme as

$$h \frac{d}{dt} \begin{bmatrix} \mathbf{u}_1 \\ \mathbf{u}_2 \\ \vdots \\ \mathbf{u}_N \end{bmatrix} + \begin{bmatrix} \mathbf{F}_{1,2} - \mathbf{F}_{1,N} \\ \mathbf{F}_{2,3} - \mathbf{F}_{2,1} \\ \vdots \\ \mathbf{F}_{N,1} - \mathbf{F}_{N,N-1} \end{bmatrix} = \mathbf{0}, \quad \mathbf{F}_{ij} = f_S(\mathbf{u}_i, \mathbf{u}_j).$$

Matrix reformulation using Hadamard products

Hadamard product of two matrices $\mathbf{A} \circ \mathbf{B}$

$$\begin{bmatrix} \mathbf{A}_{11} & \dots & \mathbf{A}_{1n} \\ \vdots & \ddots & \vdots \\ \mathbf{A}_{n1} & \dots & \mathbf{A}_{nn} \end{bmatrix} \circ \begin{bmatrix} \mathbf{B}_{11} & \dots & \mathbf{B}_{1n} \\ \vdots & \ddots & \vdots \\ \mathbf{B}_{n1} & \dots & \mathbf{B}_{nn} \end{bmatrix} = \begin{bmatrix} \mathbf{A}_{11}\mathbf{B}_{11} & \dots & \mathbf{A}_{1n}\mathbf{B}_{1n} \\ \vdots & \ddots & \vdots \\ \mathbf{A}_{n1}\mathbf{B}_{n1} & \dots & \mathbf{A}_{nn}\mathbf{B}_{nn} \end{bmatrix}.$$

Rewrite an N -point (periodic) finite volume scheme as

$$\begin{bmatrix} \mathbf{F}_{1,2} - \mathbf{F}_{1,N} \\ \mathbf{F}_{2,3} - \mathbf{F}_{2,1} \\ \vdots \\ \mathbf{F}_{N,1} - \mathbf{F}_{N,N-1} \end{bmatrix} = \left(\begin{bmatrix} 0 & 1 & -1 \\ -1 & 0 & 1 \\ \ddots & \ddots & 1 \\ 1 & -1 & 0 \end{bmatrix} \circ \begin{bmatrix} \mathbf{F}_{1,1} & \dots & \mathbf{F}_{1,N} \\ \vdots & \ddots & \vdots \\ \mathbf{F}_{N,1} & \dots & \mathbf{F}_{N,N} \end{bmatrix} \right) \mathbf{1}.$$

Matrix reformulation using Hadamard products

Hadamard product of two matrices $\mathbf{A} \circ \mathbf{B}$

$$\begin{bmatrix} \mathbf{A}_{11} & \dots & \mathbf{A}_{1n} \\ \vdots & \ddots & \vdots \\ \mathbf{A}_{n1} & \dots & \mathbf{A}_{nn} \end{bmatrix} \circ \begin{bmatrix} \mathbf{B}_{11} & \dots & \mathbf{B}_{1n} \\ \vdots & \ddots & \vdots \\ \mathbf{B}_{n1} & \dots & \mathbf{B}_{nn} \end{bmatrix} = \begin{bmatrix} \mathbf{A}_{11}\mathbf{B}_{11} & \dots & \mathbf{A}_{1n}\mathbf{B}_{1n} \\ \vdots & \ddots & \vdots \\ \mathbf{A}_{n1}\mathbf{B}_{n1} & \dots & \mathbf{A}_{nn}\mathbf{B}_{nn} \end{bmatrix}.$$

Rewrite an N -point (periodic) finite volume scheme as

$$\begin{bmatrix} \mathbf{F}_{1,2} - \mathbf{F}_{1,N} \\ \mathbf{F}_{2,3} - \mathbf{F}_{2,1} \\ \vdots \\ \mathbf{F}_{N,1} - \mathbf{F}_{N,N-1} \end{bmatrix} = \underbrace{\begin{bmatrix} 0 & 1 & -1 \\ -1 & 0 & 1 \\ \ddots & \ddots & 1 \\ 1 & -1 & 0 \end{bmatrix}}_{\text{periodic central difference}} \circ \underbrace{\begin{bmatrix} \mathbf{F}_{1,1} & \dots & \mathbf{F}_{1,N} \\ \vdots & \ddots & \vdots \\ \mathbf{F}_{N,1} & \dots & \mathbf{F}_{N,N} \end{bmatrix}}_{\text{flux matrix } \mathbf{F}} \quad 1.$$

Matrix reformulation using Hadamard products

Hadamard product of two matrices $\mathbf{A} \circ \mathbf{B}$

$$\begin{bmatrix} \mathbf{A}_{11} & \dots & \mathbf{A}_{1n} \\ \vdots & \ddots & \vdots \\ \mathbf{A}_{n1} & \dots & \mathbf{A}_{nn} \end{bmatrix} \circ \begin{bmatrix} \mathbf{B}_{11} & \dots & \mathbf{B}_{1n} \\ \vdots & \ddots & \vdots \\ \mathbf{B}_{n1} & \dots & \mathbf{B}_{nn} \end{bmatrix} = \begin{bmatrix} \mathbf{A}_{11}\mathbf{B}_{11} & \dots & \mathbf{A}_{1n}\mathbf{B}_{1n} \\ \vdots & \ddots & \vdots \\ \mathbf{A}_{n1}\mathbf{B}_{n1} & \dots & \mathbf{A}_{nn}\mathbf{B}_{nn} \end{bmatrix}.$$

Rewrite an N -point (periodic) finite volume scheme as

$$\begin{bmatrix} \mathbf{F}_{1,2} - \mathbf{F}_{1,N} \\ \mathbf{F}_{2,3} - \mathbf{F}_{2,1} \\ \vdots \\ \mathbf{F}_{N,1} - \mathbf{F}_{N,N-1} \end{bmatrix} = 2(\mathbf{Q} \circ \mathbf{F})\mathbf{1}.$$

Interpretation using finite difference matrices

Let $\mathbf{M} = h\mathbf{I}$. Can reformulate entropy conservative finite volume as

$$\mathbf{M} \frac{d\mathbf{u}}{dt} + 2(\mathbf{Q} \circ \mathbf{F}) \mathbf{1} = \mathbf{0}, \quad \mathbf{Q} = \frac{1}{2} \begin{bmatrix} 0 & 1 & & -1 \\ -1 & 0 & 1 & \\ & \ddots & \ddots & 1 \\ 1 & & -1 & 0 \end{bmatrix}$$

Note: $\mathbf{M}^{-1}\mathbf{Q}$ is a 2nd order (periodic) differentiation matrix.

Key result: generalizable beyond finite volumes

Entropy conservation for any $\underbrace{\mathbf{Q} = -\mathbf{Q}^T}_{\text{skew-symmetry}}$ and $\underbrace{\mathbf{Q}\mathbf{1} = \mathbf{0}}_{\text{conservative}}$!

Interpretation using finite difference matrices

Let $\mathbf{M} = h\mathbf{I}$. Can reformulate entropy conservative finite volume as

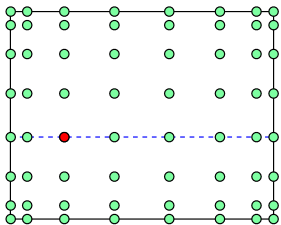
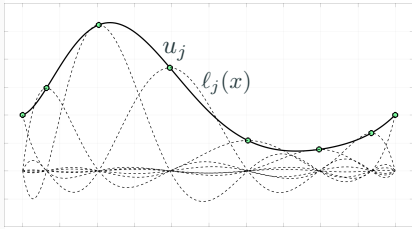
$$\mathbf{M} \frac{d\mathbf{u}}{dt} + 2(\mathbf{Q} \circ \mathbf{F}) \mathbf{1} = \mathbf{0}, \quad \mathbf{Q} = \frac{1}{2} \begin{bmatrix} 0 & 1 & & -1 \\ -1 & 0 & 1 & \\ & \ddots & \ddots & 1 \\ 1 & & -1 & 0 \end{bmatrix}$$

Note: $\mathbf{M}^{-1}\mathbf{Q}$ is a 2nd order (periodic) differentiation matrix.

Key result: generalizable beyond finite volumes

Entropy conservation for any $\underbrace{\mathbf{Q} = -\mathbf{Q}^T}_{\text{skew-symmetry}}$ and $\underbrace{\mathbf{Q}\mathbf{1} = \mathbf{0}}_{\text{conservative}}$!

Discontinuous Galerkin spectral element methods (DGSEM)



- Define weak differentiation matrix \mathbf{Q} , face extraction matrix \mathbf{E}

$$\mathbf{Q}_{ij} = \int_{-1}^1 \frac{\partial \ell_j(x)}{\partial x} \ell_i(x), \quad \mathbf{E} = \begin{bmatrix} 1 & 0 & \dots & 0 \\ 0 & \dots & 0 & 1 \end{bmatrix}.$$

- Can show \mathbf{Q} is **conservative** and has the **summation-by-parts (SBP) property** under Lobatto quadrature.

$$\boxed{\mathbf{Q}\mathbf{1} = \mathbf{0}, \quad \mathbf{Q} + \mathbf{Q}^T = \mathbf{E}^T \mathbf{B} \mathbf{E}}, \quad \mathbf{B} = \begin{bmatrix} -1 & 0 \\ 0 & 1 \end{bmatrix}.$$

Extension to multiple elements

- Let \mathbf{M} be a diagonal mass matrix, \mathbf{Q} be a conservative ($\mathbf{Q}\mathbf{1} = \mathbf{0}$) SBP operator. DG formulation:

$$\mathbf{M} \frac{d\mathbf{u}}{dt} + 2(\mathbf{Q} \circ \mathbf{F}) \mathbf{1} + \mathbf{E}^T \mathbf{B} \underbrace{\left(\mathbf{f}^*(\mathbf{u}^+, \mathbf{u}) - \mathbf{f}(\mathbf{u}) \right)}_{\text{interface flux}} = \mathbf{0}.$$

- For an entropy stable interface flux, a quadrature version of the local (cell) entropy inequality holds:

$$\int_{D^k} \frac{\partial S(u)}{\partial t} + \int_{\partial D^k} \left(\mathbf{v}^T \mathbf{f}^* - \psi(u) \right) n \leq 0.$$

Extension to multiple elements

- Let \mathbf{M} be a diagonal mass matrix, \mathbf{Q} be a conservative ($\mathbf{Q}\mathbf{1} = \mathbf{0}$) SBP operator. DG formulation:

$$\mathbf{M} \frac{d\mathbf{u}}{dt} + 2(\mathbf{Q} \circ \mathbf{F}) \mathbf{1} + \mathbf{E}^T \mathbf{B} \underbrace{\left(\mathbf{f}^*(\mathbf{u}^+, \mathbf{u}) - \mathbf{f}(\mathbf{u}) \right)}_{\text{interface flux}} = \mathbf{0}.$$

- For an entropy stable interface flux, a quadrature version of the local (cell) entropy inequality holds:

$$\boxed{\int_{D^k} \frac{\partial S(\mathbf{u})}{\partial t} + \int_{\partial D^k} \left(\mathbf{v}^T \mathbf{f}^* - \psi(\mathbf{u}) \right) n \leq 0.}$$

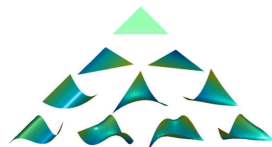
From entropy stable finite volumes to entropy stable nodal DG

“Modal” entropy stable DG formulations

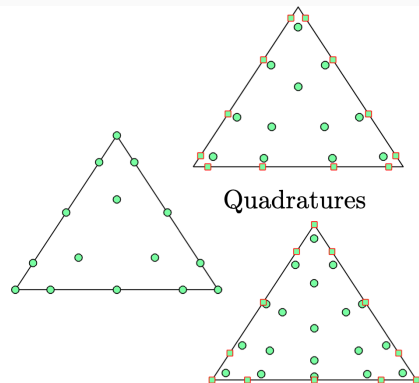
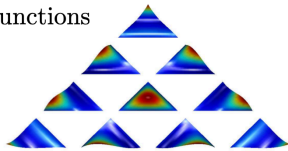
What is a “modal” formulation?

Nodal formulations: collocation, specific nodes and basis.

“Modal” formulations: arbitrary basis functions and quadrature.



Basis functions

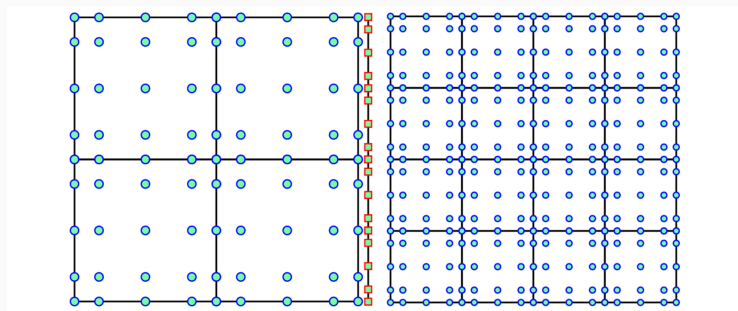


Enables standard finite element tools, recovers existing schemes.

What is a “modal” formulation?

Nodal formulations: collocation, specific nodes and basis.

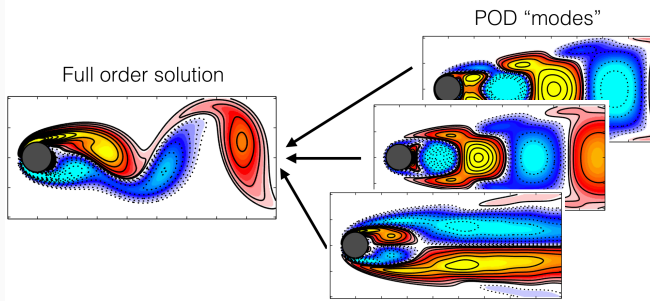
“Modal” formulations: arbitrary basis functions and quadrature.



Modal formulations make non-conforming meshes simpler.

What is a “modal” formulation?

Nodal formulations: collocation, specific nodes and basis.
“Modal” formulations: arbitrary basis functions and quadrature.



Projection-based reduced order models: learn basis functions from data.

Figure adapted from Brunton, Proctor, Kutz (2016), *Discovering governing equations from data* . . .

Chan (2020). *Entropy stable reduced order modeling of nonlinear conservation laws*.

Chan, Bencomo, Del Rey Fernandez (2020). *Mortar-based entropy-stable discontinuous Galerkin methods on non-conforming quadrilateral and hexahedral meshes*.

Nodal to modal DG: proving entropy stability

- Want a discrete version of the local entropy identity:

$$\int_{-1}^1 \mathbf{v}^T \frac{\partial \mathbf{f}(\mathbf{u})}{\partial x} = \mathbf{v}^T \mathbf{f}(\mathbf{u}) - \psi(\mathbf{u}) \Big|_{-1}^1$$

$$\mathbf{v}^T (2\mathbf{Q} \circ \mathbf{F}) \mathbf{1} = \mathbf{1}^T \mathbf{B} \left(\mathbf{v}^T \mathbf{f}(\mathbf{u}) - \psi(\mathbf{u}) \right)$$

- Key step: use nodal values of conservative/entropy variables and property of entropy conservative fluxes

$$\mathbf{v}^T \left((\mathbf{Q} - \mathbf{Q}^T) \circ \mathbf{F} \right) \mathbf{1} = \sum_{ij} \mathbf{Q}_{ij} \underbrace{(\mathbf{v}_i - \mathbf{v}_j)^T \mathbf{f}_S(\mathbf{u}_i, \mathbf{u}_j)}_{\psi(\mathbf{u}_i) - \psi(\mathbf{u}_j)}$$

Generalization to modal formulations: entropy projection

- Let \mathbf{u}_N be a degree N polynomial. Test functions must be polynomial; entropy variables $\mathbf{v}(\mathbf{u}_N)$ are not.
- Testing with L^2 projection of entropy variables $\Pi_N \mathbf{v}(\mathbf{u}_N)$ recovers rate of change of entropy:

$$\int_{D^k} \Pi_N \mathbf{v}(\mathbf{u}_N)^T \frac{\partial \mathbf{u}_N}{\partial t} = \int_{D^k} \underbrace{\mathbf{v}(\mathbf{u}_N)^T}_{\frac{\partial S(\mathbf{u})}{\partial \mathbf{u}}} \frac{\partial \mathbf{u}_N}{\partial t} = \int_{D^k} \frac{\partial S(\mathbf{u}_N)}{\partial t}$$

- For consistency, must also evaluate fluxes using projected entropy variables $\tilde{\mathbf{u}} = \mathbf{u}(\Pi_N \mathbf{v}(\mathbf{u}_N))$.

$$(\mathbf{v}_i - \mathbf{v}_j)^T \mathbf{f}_S(\mathbf{u}_i, \mathbf{u}_j) \neq \psi(\mathbf{u}_i) - \psi(\mathbf{u}_j) \quad \text{if } \mathbf{v}_i \neq \mathbf{v}(\mathbf{u}_i).$$

“Hybridization” for efficient interface coupling

- Hybridized SBP operators involve both volume/face nodes.

$$\mathbf{Q}_h = \frac{1}{2} \begin{bmatrix} \mathbf{Q} - \mathbf{Q}^T & \mathbf{E}^T \mathbf{B} \\ -\mathbf{B} \mathbf{E} & \mathbf{B} \end{bmatrix},$$

- Let $g(x)$ be a function. We can approximate $\frac{\partial g}{\partial x}$ via

$$\frac{\partial g}{\partial x} \approx \mathbf{M}^{-1} \begin{bmatrix} \mathbf{V}_q \\ \mathbf{V}_f \end{bmatrix}^T \mathbf{Q}_h \begin{bmatrix} g(\mathbf{x}_q) \\ g(\mathbf{x}_f) \end{bmatrix},$$

where $\mathbf{x}_q, \mathbf{x}_f$ are volume and face nodes, $\mathbf{V}_q, \mathbf{V}_f$ are volume and face interpolation matrices.

- Equivalent to adding error-reducing correction terms of the form “ $\mathbf{E}f(\mathbf{u}) - f(\mathbf{Eu})$ ”.

Entropy stable schemes using hybridized SBP operators

- Replace SBP operator with hybridized SBP operator

$$\mathbf{M} \frac{d\mathbf{u}}{dt} + \mathbf{2}(\mathbf{Q} \circ \mathbf{F}) \mathbf{1} + \mathbf{E}^T \mathbf{B} (\mathbf{f}^* - \mathbf{f}(\mathbf{u})) = 0.$$

- \mathbf{F} is the matrix of flux evaluations using solution values at *both* volume and face nodes + entropy projection:

$$\mathbf{F}_{ij} = f_S(\tilde{\mathbf{u}}_i, \tilde{\mathbf{u}}_j), \quad \tilde{\mathbf{u}} = \text{evaluate } \mathbf{u}(\Pi_N \mathbf{v}(\mathbf{u})).$$

- Entropy stable if $\mathbf{Q}_h \mathbf{1} = \mathbf{0}$ (true under weak conditions on quadrature accuracy).

Entropy stable schemes using hybridized SBP operators

- Replace SBP operator with hybridized SBP operator

$$\mathbf{M} \frac{d\mathbf{u}}{dt} + 2 \begin{bmatrix} \mathbf{V}_q \\ \mathbf{V}_f \end{bmatrix}^T (\mathbf{Q}_h \circ \mathbf{F}) \mathbf{1} + \mathbf{V}_f^T \mathbf{B} (\mathbf{f}^* - \mathbf{f}(\mathbf{u})) = 0.$$

- \mathbf{F} is the matrix of flux evaluations using solution values at *both* volume and face nodes + entropy projection:

$$\mathbf{F}_{ij} = \mathbf{f}_S(\tilde{\mathbf{u}}_i, \tilde{\mathbf{u}}_j), \quad \tilde{\mathbf{u}} = \text{evaluate } \mathbf{u}(\Pi_N v(\mathbf{u})).$$

- Entropy stable if $\mathbf{Q}_h \mathbf{1} = \mathbf{0}$ (true under weak conditions on quadrature accuracy).

Entropy stable schemes using hybridized SBP operators

- Replace SBP operator with hybridized SBP operator

$$\mathbf{M} \frac{d\mathbf{u}}{dt} + 2 \begin{bmatrix} \mathbf{V}_q \\ \mathbf{V}_f \end{bmatrix}^T (\mathbf{Q}_h \circ \mathbf{F}) \mathbf{1} + \mathbf{V}_f^T \mathbf{B} (\mathbf{f}^* - \mathbf{f}(\mathbf{u})) = 0.$$

- \mathbf{F} is the matrix of flux evaluations using solution values at *both* volume and face nodes + **entropy projection**:

$$\mathbf{F}_{ij} = \mathbf{f}_S(\tilde{\mathbf{u}}_i, \tilde{\mathbf{u}}_j), \quad \tilde{\mathbf{u}} = \text{evaluate } \mathbf{u}(\Pi_N \mathbf{v}(\mathbf{u})).$$

- Entropy stable if $\mathbf{Q}_h \mathbf{1} = \mathbf{0}$ (true under weak conditions on quadrature accuracy).

Entropy stable schemes using hybridized SBP operators

- Replace SBP operator with hybridized SBP operator

$$\mathbf{M} \frac{d\mathbf{u}}{dt} + 2 \begin{bmatrix} \mathbf{V}_q \\ \mathbf{V}_f \end{bmatrix}^T (\mathbf{Q}_h \circ \mathbf{F}) \mathbf{1} + \mathbf{V}_f^T \mathbf{B} (\mathbf{f}^* - \mathbf{f}(\mathbf{u})) = 0.$$

- \mathbf{F} is the matrix of flux evaluations using solution values at *both* volume and face nodes + **entropy projection**:

$$\mathbf{F}_{ij} = \mathbf{f}_S(\tilde{\mathbf{u}}_i, \tilde{\mathbf{u}}_j), \quad \tilde{\mathbf{u}} = \text{evaluate } \mathbf{u}(\Pi_N \mathbf{v}(\mathbf{u})).$$

- Entropy stable if $\mathbf{Q}_h \mathbf{1} = \mathbf{0}$ (true under weak conditions on quadrature accuracy).

Building on modal entropy stable formulations

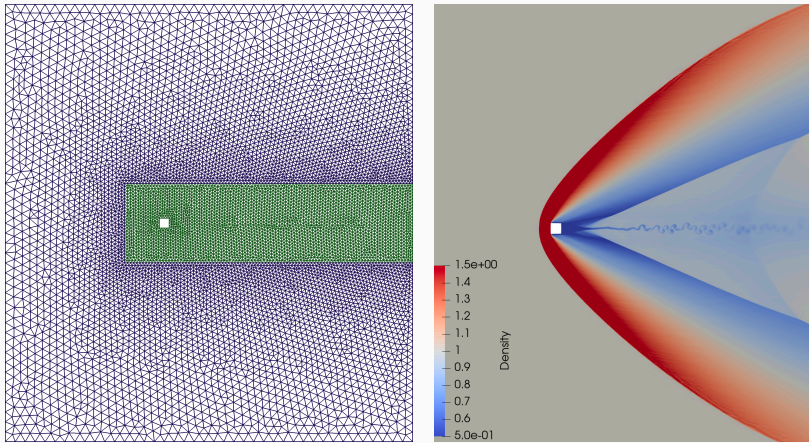
Over the last few years:

- Entropy stable reduced order modeling
- Non-conforming meshes (Mario Bencomo, DCDR Fernandez)
- Networks and multi-dimensional domains (Philip Wu)
- Compressible Navier-Stokes (Yimin Lin, T. Warburton)
- Quasi-1D equations (Charlie Liu, Philip Wu)
- Robust high order DG for under-resolved flows

Other work applicable to traditional entropy stable SBP schemes:

- Fast computation of Jacobian matrices (Christina Taylor)
- Positivity preserving schemes (Philip Wu, Yimin Lin, et al)

Compressible Navier-Stokes: flow over a square cylinder

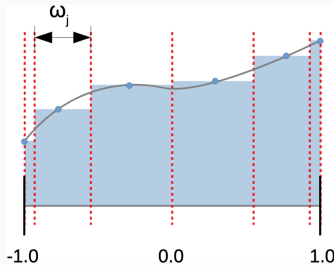


Density at $T_{\text{final}} = 100$ for $\text{Re} = 10^4$, $\text{Ma} = 1.5$ for a degree $N = 3$ mesh with 16,574 elements. Discretization of diffusive terms: symmetrization of viscous fluxes, stable imposition of wall boundary conditions.

Positivity preserving entropy stable nodal DG for the compressible Navier-Stokes equations

Entropy stability requires positivity

Entropy stable schemes require positivity of density, pressure (numerical fluxes depend on *logarithm* of density, temperature).



Interpretation of Lobatto nodes as a sub-cell finite volume grid.

- Hard to enforce both high order accuracy and positivity.
- Strategy: enforce positivity while retaining **subcell resolution**.

Enforcing positivity: a low order subcell scheme

Restricted to **nodal** methods (e.g., mass lumping, collocation).

Global formulation using forward Euler (higher order via SSP-RK).

Let $\mathbf{Q}_{ij} = -\mathbf{Q}_{ij}$, $\mathbf{f}_j = \mathbf{f}(\mathbf{u}_j)$, and $\mathbf{d}_{ij} = \mathbf{d}_{ji} > 0$

$$\mathbf{m}_i \frac{\mathbf{u}_i^{k+1} - \mathbf{u}_i}{\Delta t} + \sum_j \mathbf{Q}_{ij} \mathbf{f}_j - \underbrace{\mathbf{d}_{ij} (\mathbf{u}_j - \mathbf{u}_i)}_{\text{algebraic dissipation}} = 0.$$

Use **conservation**, **SBP** properties to rewrite using “bar states”

$$\bar{\mathbf{u}}_{ij} = \frac{1}{2} (\mathbf{u}_i + \mathbf{u}_j) - \frac{\mathbf{Q}_{ij}}{\mathbf{d}_{ij}} (\mathbf{f}_j - \mathbf{f}_i).$$

$$\frac{\mathbf{m}_i}{\Delta t} \mathbf{u}_i^{k+1} = \left(\frac{\mathbf{m}_i}{\Delta t} - \sum_{j \neq i} 2\mathbf{d}_{ij} \right) \mathbf{u}_i + \sum_{j \neq i} \frac{2\Delta t \mathbf{d}_{ij}}{\mathbf{m}_i} \bar{\mathbf{u}}_{ij}.$$

Enforcing positivity: a low order subcell scheme

Restricted to **nodal** methods (e.g., mass lumping, collocation).

Global formulation using forward Euler (higher order via SSP-RK).

Let $\mathbf{Q}_{ij} = -\mathbf{Q}_{ij}$, $\mathbf{f}_j = \mathbf{f}(\mathbf{u}_j)$, and $\mathbf{d}_{ij} = \mathbf{d}_{ji} > 0$

$$\mathbf{m}_i \frac{\mathbf{u}_i^{k+1} - \mathbf{u}_i}{\Delta t} + \sum_j \mathbf{Q}_{ij} \mathbf{f}_j - \underbrace{\mathbf{d}_{ij} (\mathbf{u}_j - \mathbf{u}_i)}_{\text{algebraic dissipation}} = \mathbf{0}.$$

Use **conservation**, **SBP** properties to rewrite using “bar states”

$$\bar{\mathbf{u}}_{ij} = \frac{1}{2} (\mathbf{u}_i + \mathbf{u}_j) - \frac{\mathbf{Q}_{ij}}{\mathbf{d}_{ij}} (\mathbf{f}_j - \mathbf{f}_i).$$

$$\frac{\mathbf{m}_i}{\Delta t} \mathbf{u}_i^{k+1} = \left(\frac{\mathbf{m}_i}{\Delta t} - \sum_{j \neq i} 2\mathbf{d}_{ij} \right) \mathbf{u}_i + \sum_{j \neq i} \frac{2\Delta t \mathbf{d}_{ij}}{\mathbf{m}_i} \bar{\mathbf{u}}_{ij}.$$

Enforcing positivity: a low order subcell scheme

Restricted to **nodal** methods (e.g., mass lumping, collocation).

Global formulation using forward Euler (higher order via SSP-RK).

Let $\mathbf{Q}_{ij} = -\mathbf{Q}_{ij}$, $\mathbf{f}_j = \mathbf{f}(\mathbf{u}_j)$, and $\mathbf{d}_{ij} = \mathbf{d}_{ji} > 0$

$$\mathbf{m}_i \frac{\mathbf{u}_i^{k+1} - \mathbf{u}_i}{\Delta t} + \sum_j \mathbf{Q}_{ij} \mathbf{f}_j - \underbrace{\mathbf{d}_{ij} (\mathbf{u}_j - \mathbf{u}_i)}_{\text{algebraic dissipation}} = \mathbf{0}.$$

Use **conservation**, **SBP** properties to rewrite using “bar states”

$$\bar{\mathbf{u}}_{ij} = \frac{1}{2} (\mathbf{u}_i + \mathbf{u}_j) - \frac{\mathbf{Q}_{ij}}{\mathbf{d}_{ij}} (\mathbf{f}_j - \mathbf{f}_i).$$

$$\frac{\mathbf{m}_i}{\Delta t} \mathbf{u}_i^{k+1} = \left(\frac{\mathbf{m}_i}{\Delta t} - \sum_{j \neq i} 2\mathbf{d}_{ij} \right) \mathbf{u}_i + \sum_{j \neq i} \frac{2\Delta t \mathbf{d}_{ij}}{\mathbf{m}_i} \bar{\mathbf{u}}_{ij}.$$

Provable positivity under a CFL condition

- Bar states $\bar{\mathbf{u}}_{ij}$ **preserve positivity** for \mathbf{d}_{ij} sufficiently large

$$\bar{\mathbf{u}}_{ij} = \frac{1}{2} (\mathbf{u}_i + \mathbf{u}_j) - \frac{\mathbf{Q}_{ij}}{\mathbf{d}_{ij}} (\mathbf{f}_j - \mathbf{f}_i), \quad \mathbf{d}_{ij} \geq \lambda_{\max}(\mathbf{u}_i, \mathbf{u}_j, \mathbf{Q}_{ij}).$$

- \mathbf{u}_i^{k+1} is positive (e.g., convex combination of \mathbf{u}_i and $\bar{\mathbf{u}}_{ij}$) if

$$\Delta t \leq \min_i \frac{\mathbf{m}_i}{2 \sum_{i \neq j} \mathbf{d}_{ij}}.$$

Extension to compressible Navier-Stokes

- Entropy stable low order discretization of first order form of viscous terms $\boldsymbol{\sigma} = \text{stress } \boldsymbol{\tau} + \text{heat conduction } q$.

$$\mathbf{M} \frac{d\mathbf{u}}{dt} + \sum_j \mathbf{Q}_{ij} (\mathbf{f}_j - \boldsymbol{\sigma}_j) - \mathbf{d}_{ij} (\mathbf{u}_j - \mathbf{u}_i) = \mathbf{0}.$$

- Reformulate scheme in terms of viscous bar states:

$$\bar{\mathbf{u}}_{ij} = \frac{1}{2} (\mathbf{u}_i + \mathbf{u}_j) - \frac{\mathbf{Q}_{ij}}{\mathbf{d}_{ij}} ((\mathbf{f}_j - \boldsymbol{\sigma}_j) - (\mathbf{f}_i - \boldsymbol{\sigma}_i))$$

- Positivity of ρ, p under a (viscous) CFL condition with

$$\mathbf{d}_{ij} = \max(\beta(\mathbf{u}_i), \beta(\mathbf{u}_j), \lambda_{\max}(\mathbf{u}_i, \mathbf{u}_j, \mathbf{Q}_{ij}), \lambda_{\max}(\mathbf{u}_j, \mathbf{u}_i, \mathbf{Q}_{ji}))$$

$$\beta(u) > |v \cdot n| + \frac{1}{2\rho^2 e} \left(\sqrt{\rho^2 (q \cdot n)^2 + 2\rho^2 e \|\boldsymbol{\tau} \cdot n - pn\|} \right) + \rho |q \cdot n|$$

Extension to compressible Navier-Stokes

- Entropy stable low order discretization of first order form of viscous terms $\boldsymbol{\sigma} = \text{stress } \boldsymbol{\tau} + \text{heat conduction } q$.

$$\mathbf{M} \frac{d\mathbf{u}}{dt} + \sum_j \mathbf{Q}_{ij} (\mathbf{f}_j - \boldsymbol{\sigma}_j) - \mathbf{d}_{ij} (\mathbf{u}_j - \mathbf{u}_i) = \mathbf{0}.$$

- Reformulate scheme in terms of viscous bar states:

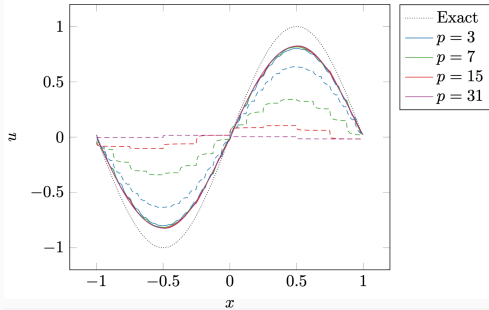
$$\bar{\mathbf{u}}_{ij} = \frac{1}{2} (\mathbf{u}_i + \mathbf{u}_j) - \frac{\mathbf{Q}_{ij}}{\mathbf{d}_{ij}} ((\mathbf{f}_j - \boldsymbol{\sigma}_j) - (\mathbf{f}_i - \boldsymbol{\sigma}_i))$$

- Positivity of ρ, p under a (viscous) CFL condition with

$$\mathbf{d}_{ij} = \max(\beta(\mathbf{u}_i), \beta(\mathbf{u}_j), \lambda_{\max}(\mathbf{u}_i, \mathbf{u}_j, \mathbf{Q}_{ij}), \lambda_{\max}(\mathbf{u}_j, \mathbf{u}_i, \mathbf{Q}_{ji}))$$

$$\beta(\mathbf{u}) > |\mathbf{v} \cdot \mathbf{n}| + \frac{1}{2\rho^2 e} \left(\sqrt{\rho^2(\mathbf{q} \cdot \mathbf{n})^2 + 2\rho^2 e \|\boldsymbol{\tau} \cdot \mathbf{n} - p\mathbf{n}\|} \right) + \rho |\mathbf{q} \cdot \mathbf{n}|$$

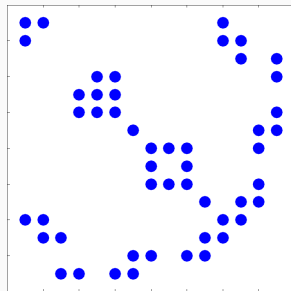
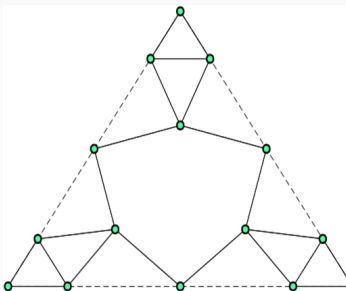
Sparsification of low order matrices



Effect of sparsification on solution dissipation; figure taken from Pazner (2021).

- **Algebraic** artificial dissipation depends on discretization matrices \Rightarrow dense operators produce too much diffusion!
- New sparsified operators on simplicial elements inspired by the construction of meshfree methods.

Sparsification of low order matrices



- **Algebraic** artificial dissipation depends on discretization matrices \Rightarrow dense operators produce too much diffusion!
- New sparsified operators on simplicial elements inspired by the construction of meshfree methods.

Sparse low order approximations to simplicial SBP operators

- Want to preserve conservation
 $\mathbf{Q}^{\text{low}} \mathbf{1} = \mathbf{0}$ and SBP property

$$\mathbf{Q}^{\text{low}} + (\mathbf{Q}^{\text{low}})^T = \mathbf{B}.$$

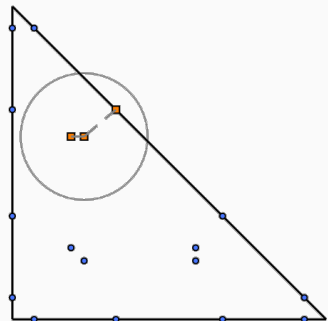
- For neighboring i and j , assume

$$(\mathbf{Q}^{\text{low}} - (\mathbf{Q}^{\text{low}})^T)_{ij} = \psi_j - \psi_i.$$

- Enforcing $\mathbf{Q}^{\text{low}} \mathbf{1} = \mathbf{0}$ equivalent to

$$\sum_j \psi_j - \psi_i = \left(-\frac{1}{2} \mathbf{B} \mathbf{1} \right)_i,$$

$$\text{s.t. } \boldsymbol{\psi}^T \mathbf{1} = 0.$$



Quadrature nodes from Chen, Shu (2017) for a degree $N = 3$ SBP operator. The sparse low order operator \mathbf{Q}^{low} uses the same nodes and weights.

Blending high and low order DG solutions

- Blend high and low order solutions over each element to retain accuracy where possible while ensuring positivity.

$$\mathbf{u}^{k+1} = (1 - \ell)\mathbf{u}^{k+1,\text{low}} + \ell\mathbf{u}^{k+1,\text{high}}$$

- Impose relaxed local bounds based on low order solution

$$\rho \geq \alpha \rho^{\text{low}}, \quad p \geq \alpha p^{\text{low}}, \quad \alpha \in [0, 1].$$

- Local entropy inequality: preserved for element-wise blending.
- Local conservation: preserved if high and low order schemes use the same interface flux.

Convergence tests: LeBlanc and viscous shock tube

h	$N = 2$		$N = 5$	
	L^1 error	Rate	L^1 error	Rate
0.02	8.681×10^{-2}		5.956×10^{-2}	.
0.01	3.658×10^{-2}	1.25	1.436×10^{-2}	2.05
0.005	1.329×10^{-2}	1.46	3.630×10^{-3}	1.98
0.0025	6.015×10^{-3}	1.14	1.129×10^{-3}	1.69
0.00125	2.910×10^{-3}	1.05	5.889×10^{-4}	0.94

(a) Leblanc shock tube, bound relaxation $\alpha = 0.5$

h	$N = 2$		$N = 3$	
	L^1 error	Rate	L^1 error	Rate
0.025	2.305×10^{-2}		2.071×10^{-2}	
0.0125	9.858×10^{-3}	1.23	6.749×10^{-3}	1.62
0.00625	3.382×10^{-3}	1.54	1.278×10^{-3}	2.40
0.003125	5.765×10^{-4}	2.55	1.163×10^{-4}	3.45
0.0015625	8.836×10^{-5}	2.71	1.269×10^{-5}	3.20

(b) 1D viscous shock, $Re = 1000$, bound relaxation $\alpha = 0.5$

Viscous shock is run at Mach 20 to generate positivity violations.

Isentropic vortex with small minimum density

h	$N = 2$		$N = 3$		$N = 4$	
	L^2 error	Rate	L^2 error	Rate	L^2 error	Rate
2.5	1.148×10^0		5.958×10^{-1}	1.28	4.073×10^{-1}	
1.25	4.865×10^{-1}	1.24	1.905×10^{-1}	1.64	8.987×10^{-2}	2.18
0.625	1.223×10^{-1}	1.99	2.308×10^{-2}	3.05	1.511×10^{-2}	2.57
0.3125	1.706×10^{-2}	2.84	2.393×10^{-3}	3.27	1.915×10^{-4}	6.30

(c) Quadrilateral meshes, bound relaxation $\alpha = 0.5$

h	$N = 2$		$N = 3$		$N = 4$	
	L^2 error	Rate	L^2 error	Rate	L^2 error	Rate
2.5	7.887×10^{-1}		5.034×10^{-1}		4.059×10^{-1}	
1.25	3.834×10^{-1}	1.04	1.881×10^{-1}	1.42	9.890×10^{-2}	2.04
0.625	8.993×10^{-2}	2.09	2.944×10^{-2}	2.68	1.578×10^{-2}	2.65
0.3125	1.298×10^{-2}	2.79	2.606×10^{-3}	3.50	4.258×10^{-4}	5.21

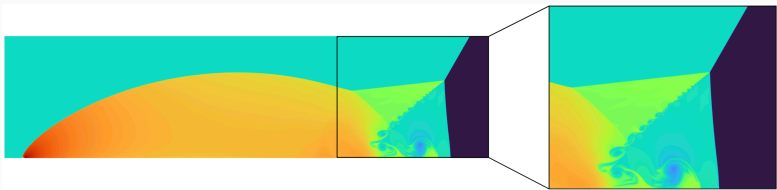
(d) Triangular meshes, bound relaxation $\alpha = 0.5$

Vortex parameters are set such that $\rho_{\min} = 2.145 \times 10^{-3}$.

Compressible Euler: double Mach reflection (Yimin Lin)



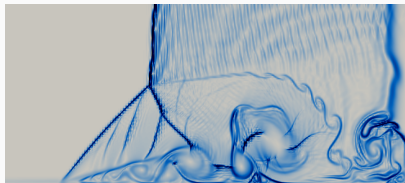
(a) Subcell positivity-preserving entropy stable nodal DG, $\alpha = 0.5$, $T = .2$



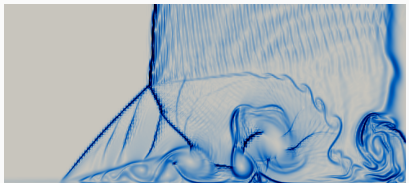
(b) Subcell invariant domain preserving nodal DG (Pazner 2021), $T = .275$

Density for $N = 3$ entropy stable DG (250×875 elements) and a reference solution (600×2400 elements). Note: positivity is sensitive to the wall boundary treatment!

Compressible Navier-Stokes: Daru-Tenaud shock tube



(a) Bound relaxation $\alpha = 0.5$



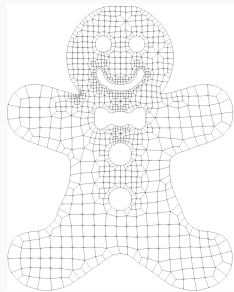
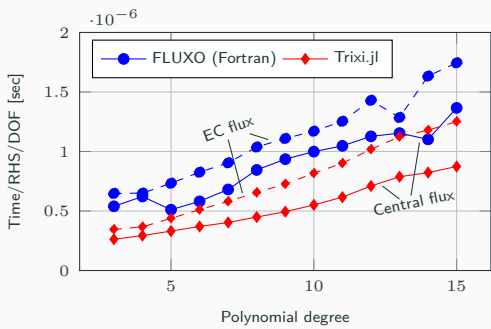
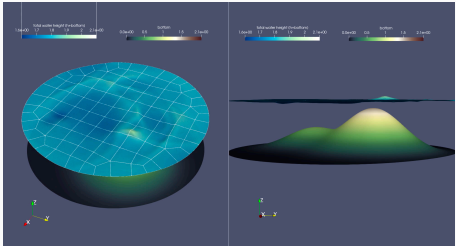
(b) Bound relaxation $\alpha = 0.1$

Numerical schlieren plots for $N = 3$, 120×240 elements, $\text{Re} = 1000$ at $T_{\text{final}} = 1$.

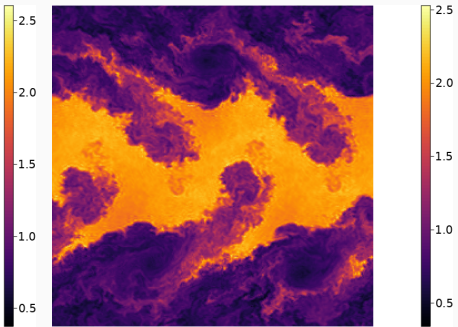
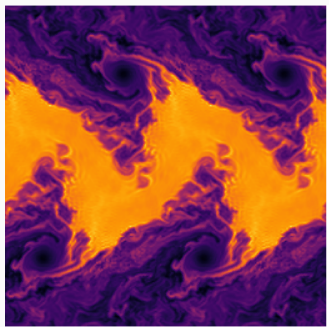
- Conjecture: oscillations related to low order scheme, which resembles Lax-Friedrichs with Davis estimate.
- Similar oscillations observed when using ESDG + LxF for shock-vortex interaction (oscillations vanish under HLLC flux).

Differences in robustness for different entropy stable schemes

In this section: Trixi.jl Julia library, adaptive explicit RK



Differences in ESDG robustness for compressible Euler



(a) Degree $N = 3$ and a 64×64 mesh. (b) Degree $N = 7$ and a 32×32 mesh.

Density at time $T = 10$ for the Kelvin-Helmholtz instability using an entropy stable DG method with entropy projection.

Differences in ESDG robustness for compressible Euler

Solver \ Degree	1	2	3	4	5	6	7
Collocation	15	4.81	3.77	4.43	3.74	3.37	3.64
Entropy projection	15	15	15	15	15	15	15

$$N_{\text{cells}} = 16$$

Solver \ Degree	1	2	3	4	5	6	7
Collocation	15	4.12	3.65	4.27	3.54	3.66	3.56
Entropy projection	15	15	15	15	15	15	15

$$N_{\text{cells}} = 32$$

End times for the Kelvin-Helmholtz instability on quadrilateral meshes.
Blue indicates stable simulations, while red indicate crashes.

Differences in ESDG robustness for compressible Euler

Solver \ Degree	1	2	3	4	5	6
Collocation	15	3.98	3.44	2.99	2.94	3.13
Entropy projection	15	15	15	15	15	15

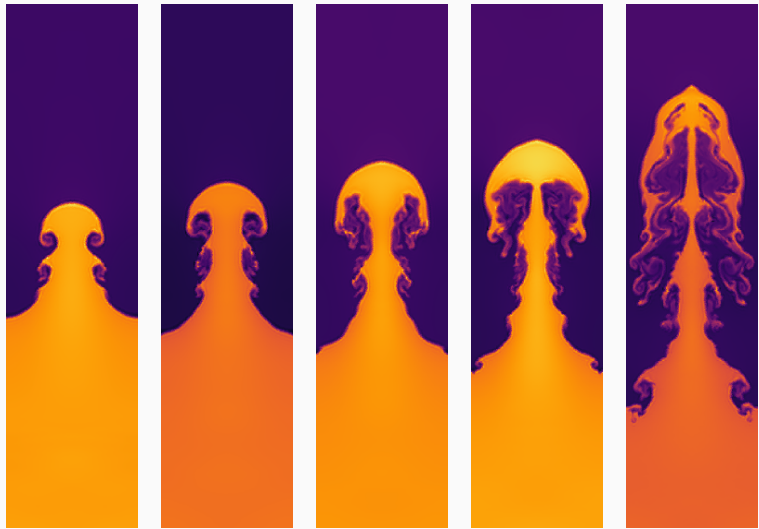
$$N_{\text{cells}} = 16$$

Solver \ Degree	1	2	3	4	5	6
Collocation	3.919	3.45	3.19	2.96	3.06	3.27
Entropy projection	15	15	15	15	15	15

$$N_{\text{cells}} = 32$$

End times for the Kelvin-Helmholtz instability on triangular meshes. Blue indicates stable simulations, while red indicate crashes.

Similar behavior for Rayleigh-Taylor, Richtmeyer-Meshkov



(a) $t = 1.25$

(b) $t = 1.5$

(c) $t = 1.75$

(d) $t = 2$

(e) $t = 2.5$

Rayleigh-Taylor instability: $N = 3$ entropy projection DG, 32×128 elements.

Similar behavior for Rayleigh-Taylor, Richtmeyer-Meshkov

Solver \ Degree	1	2	3	4	5	6	7
Collocation	3.67	3.4	3.33	3.26	3.11	3.03	3.04
Entropy projection	15	15	15	15	15	15	15

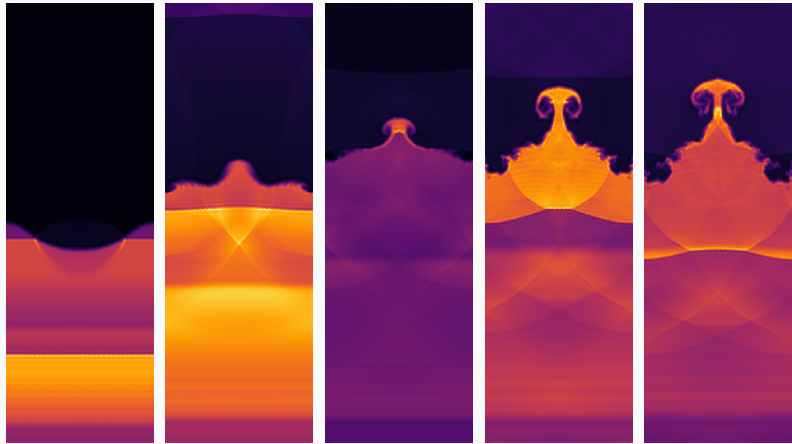
RTI, quadrilateral mesh, $N_{\text{cells}} = 16$

Solver \ Degree	1	2	3	4	5	6	7
Collocation	4.00	3.14	3.44	3.16	3.03	2.97	2.98
Entropy projection	15	15	15	15	15	15	15

RTI, quadrilateral mesh, $N_{\text{cells}} = 32$

End times for the Rayleigh-Taylor instability. Blue indicates stable simulations, while red indicate crashes.

Similar behavior for Rayleigh-Taylor, Richtmeyer-Meshkov



(a) $t = 7.5$

(b) $t = 15$

(c) $t = 20$

(d) $t = 25$

(e) $t = 27.5$

Richtmeyer-Meshkov instability using $N = 3$ entropy projection DG with 32×96 elements. Entropy projection is stable up to $T = 50$; entropy stable collocation crashes at $T \approx 20.1$.

Similar behavior for Rayleigh-Taylor, Richtmeyer-Meshkov

Solver \ Degree	1	2	3	4	5	6	7
Collocation	30	30	27.96	24.94	8.851	8.853	8.85
Entropy projection	30	30	30	30	30	30	30

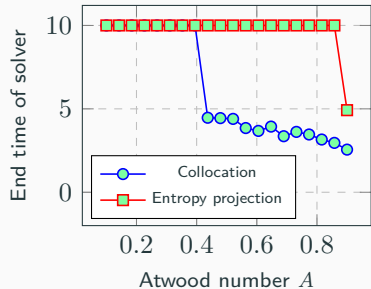
RMI, quadrilateral mesh, $N_{\text{cells}} = 16$

Solver \ Degree	1	2	3	4	5	6	7
Collocation	30	25.52	23.34	8.759	7.808	7.014	7.01
Entropy projection	30	30	30	30	30	30	30

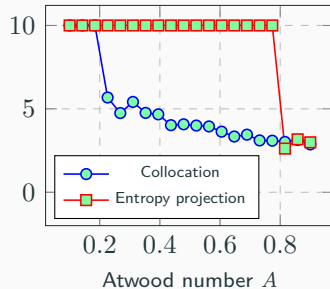
RMI, quadrilateral mesh, $N_{\text{cells}} = 32$

End times for the Richtmeyer-Meshkov instability. Blue indicates stable simulations, while red indicate crashes.

Robustness depends on the Atwood number



(a) $N = 3$, 32×32 quad mesh



(b) $N = 7$, 16×16 quad mesh

- Entropy stable collocation DG is robust when density is near-constant, but crashes at higher Atwood numbers

$$A = (\rho_2 - \rho_1)/(\rho_1 + \rho_2), \quad A \in [0, 1].$$

- Entropy projection is stable up to $A \approx .8$.

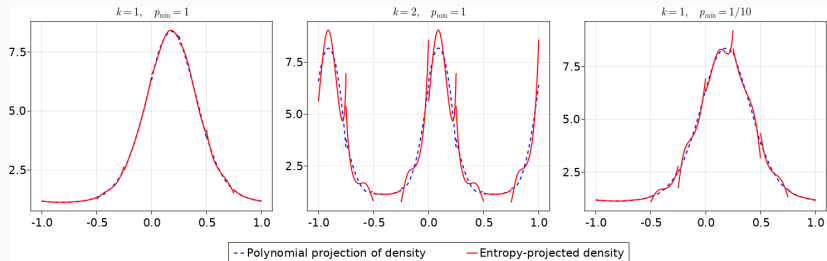
Why the difference in robustness?

CAN YOU SPOT ALL 5 DIFFERENCES BETWEEN
THESE TWO discretizations ?



- Both are entropy stable, but Gauss collocation increases quadrature accuracy (reduces aliasing).
- Gauss introduces interface corrections and **entropy projection**.

Why would the entropy projection improve robustness?



Some clues: entropy projection uses L^2 projection of entropy variables, amplifies effects of **under-resolution** and **near-zero density or pressure**.

Potential explanation: does the entropy projection activate more interface dissipation?

Improved robustness is not due to interface dissipation

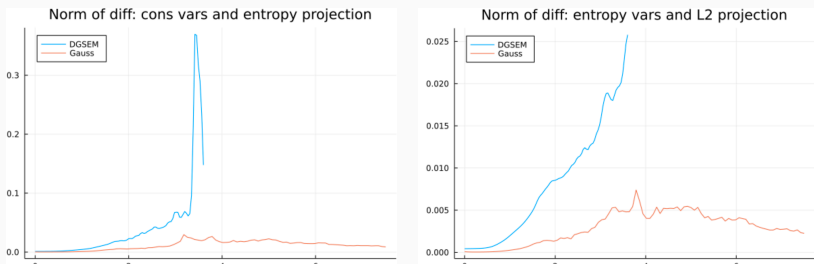
Solver \ Degree	1	2	3	4	5	6	7
Collocation	20	20	20	20	6.035	5.29	5.02
Entropy projection	20	20	20	20	20	20	20

$$N_{\text{cells}} = 8^3$$

End times for entropy *conservative* simulations of the Taylor-Green vortex on hex meshes. Blue indicates stable simulations, while red indicate crashes.

We observe differences in robustness even for *entropy conservative* schemes (no entropy dissipation).

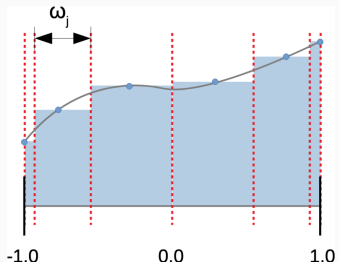
Evolution of the difference between conservative variables and entropy projected variables



Difference over time between the conservative and entropy projected variables $\|\tilde{u} - u\|_{L^2}$ for collocation and entropy projection schemes.

If $\tilde{u} \approx u$, the mapping between conservative and entropy variables is well-posed \implies the density and pressure are positive?

Why not just use shock capturing and positivity limiting?



Interpretation of Lobatto nodes as a sub-cell finite volume grid.

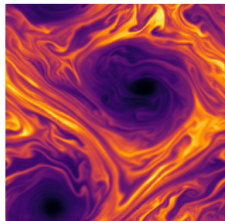
We compare entropy projection DG to two state-of-the-art schemes:

- DGSEM-SC-PP: **very light** entropy stable shock capturing + Zhang-Shu positivity limiting.
- DGSEM-subcell: positivity and shock capturing using **subcell convex limiting**.

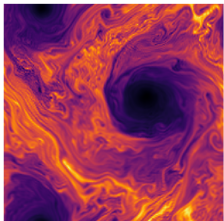
Hennemann, Ruéda-Ramírez, Hindenlang, Gassner (2021). A provably entropy stable subcell shock capturing approach for high order split form DG for the compressible Euler equations.

Ruéda-Ramírez, Pazner, Gassner (2022, preprint). Subcell limiting strategies for DGSEM.

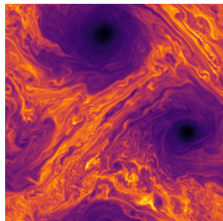
Application: under-resolved “turbulent” flows



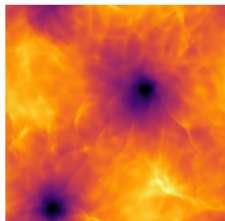
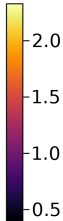
DGSEM-SC-PP density



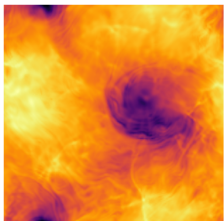
DGSEM-subcell density



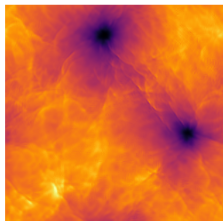
Gauss density



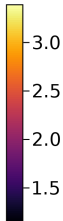
DGSEM-SC-PP pressure



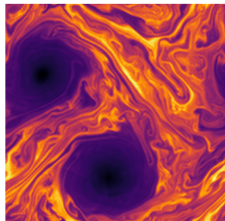
DGSEM-subcell pressure



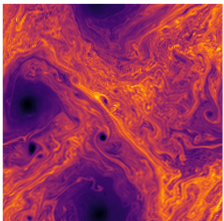
Gauss pressure



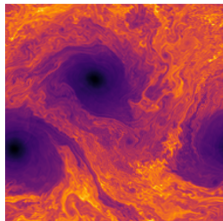
Application: under-resolved “turbulent” flows



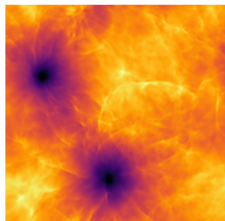
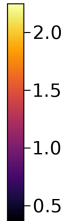
DGSEM-SC-PP density



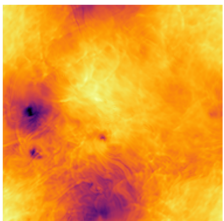
DGSEM-subcell density



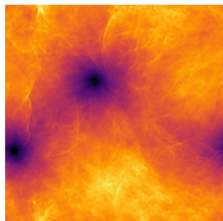
Gauss density



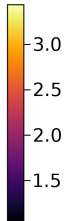
DGSEM-SC-PP pressure



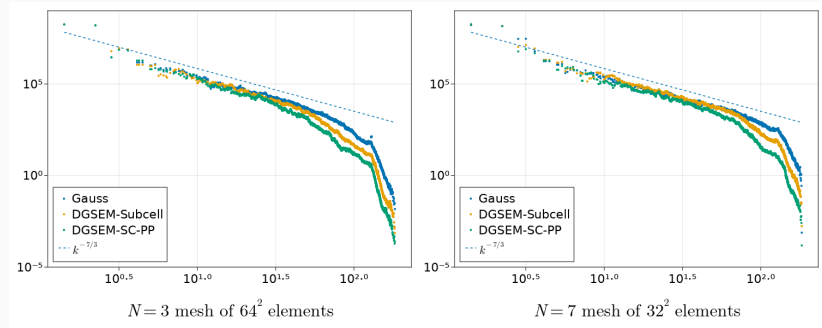
DGSEM-subcell pressure



Gauss pressure



Under-resolved “turbulence” is sensitive to extra dissipation



- Sample with $(N + 1) \times \text{number of elements}$ points (uniformly spaced to avoid element interfaces) along each dimension.
- Compute Fourier modes of velocity weighted by $\sqrt{\rho}$, sum energy over “effective wavenumbers” for a 1D power spectra.

Conclusion

- Positivity preserving limiters enable robust entropy stable nodal DG simulations of compressible flow.
- Modal entropy stable DG improves the robustness of high order DG methods for under-resolved flows.
- This work is supported by DMS-1719818 and DMS-1943186.

Thank you! Questions?



Chan, Ranocha, Rueda-Ramírez, Gassner, Warburton (2022). *On the entropy projection and the robustness of high order entropy stable discontinuous Galerkin schemes for under-resolved flows*.

Lin, Chan, Tomas (2022). *A positivity preserving strategy for entropy stable discontinuous Galerkin discretizations of the compressible Euler and Navier-Stokes equations*.

Chan, Lin, Warburton (2021). *Entropy stable modal discontinuous Galerkin schemes and wall boundary conditions for the compressible Navier-Stokes equation*.

Additional slides

Estimated cost for DGSEM and Gauss

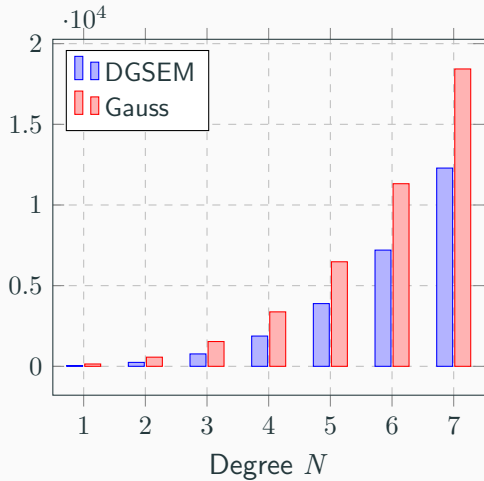
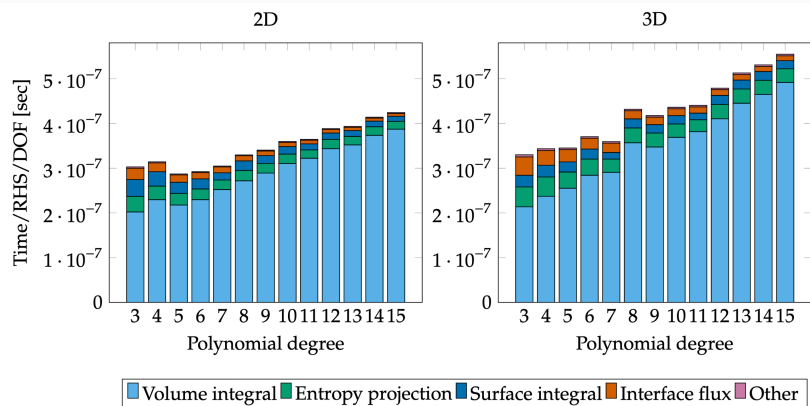


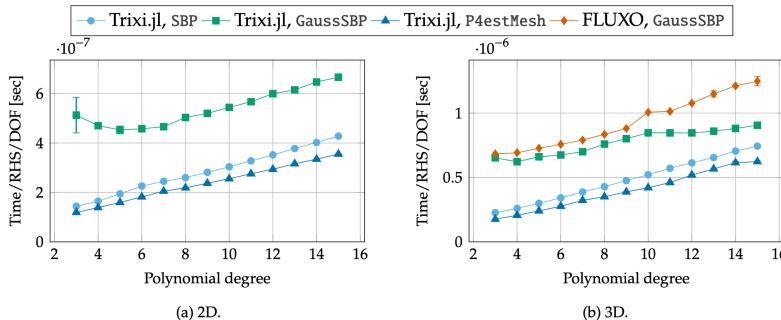
Figure 1: Comparison of 3D entropy stable DGSEM and entropy stable Gauss collocation in terms of two-point numerical flux evaluations.

Actual cost comparison for DGSEM and Gauss



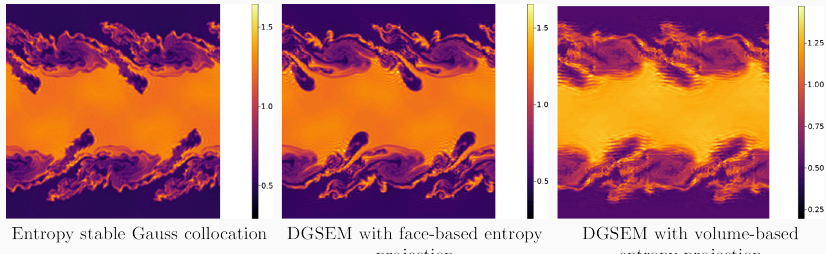
Performance index (PID) for entropy stable Gauss collocation.

Cost comparison of different implementations



Runtime per RHS evaluation for different implementations of entropy stable DGSEM and Gauss collocation.

Does the entropy projection also help “bad” DG schemes?

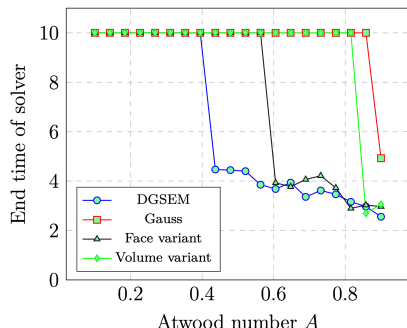


Degree $N = 3$ and 64×64 grid Kelvin-Helmholtz simulations at $T = 5$.

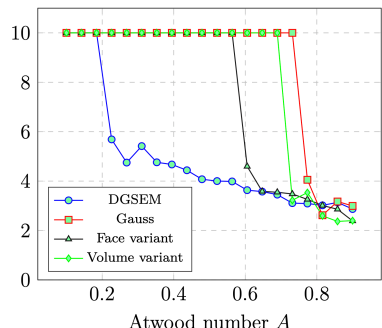
All methods run until $T = 25$, while DGSEM crashes at $T \approx 3.5$.

“Variant” schemes introduce entropy projection, but have similar or lower quadrature accuracy compared with DGSEM.

Improved robustness is not (only) due to quadrature accuracy



$N = 3, 32 \times 32$ quadrilateral mesh



$N = 7, 16 \times 16$ quadrilateral mesh

Entropy projection is not the only factor: “bad” entropy projection variant schemes improve robustness, but not as much.